

MAPBIOMAS

CHILE

Infrastructure Appendix

Algorithm Theoretical Base Document

MapBiomas "Handbook"

Executive Committee MapBiomas Chile

Jaime Hernández (U. de Chile)
Cristian Echeverria (U. de Concepción)
Adison Altamirano (U. de la Frontera)

General Coordination MapBiomas Chile

Jaime Hernández
Danniela Espinoza

Supervisory team

Jaime Hernández

Developers

Valentina González
Carlos Hormazabal
Lissette Cortés

Technical team

Diego Muñoz
Felipe Lepín
Valeria Castro

MapBiomas Brasil

Tasso Azevedo
Julia Shimbo
Marcos Rosa
Joao Siquiera
Mayra Milkovic

Index

<u>1. Introduction</u>	4
<u>1.1. Overview</u>	4
<u>2. Landsat Image Mosaics</u>	5
<u>2.1. Mosaic Composition</u>	5
<u>2.2. Feature Space</u>	5
<u>3. Classification</u>	6
<u>3.1. Definition of potential areas</u>	6
<u>3.2. Definition of the Infrastructure class (ID: 24)</u>	6
<u>3.3. Samples Collection</u>	6
<u>3.4. Working areas</u>	6
<u>3.5. Classification Algorithm</u>	7
<u>4. Post Processing</u>	9
<u>4.1. Temporal filters</u>	9
<u>4.2. First and Last year filter</u>	9
<u>4.3. Fill Gaps filter</u>	10
<u>4.4. Spatial filter</u>	10
<u>4.5. Frequency filter</u>	11
<u>4.6. Morphological filter</u>	12
<u>4.7. Remap</u>	12
<u>5. Integration</u>	12
<u>6. References</u>	14

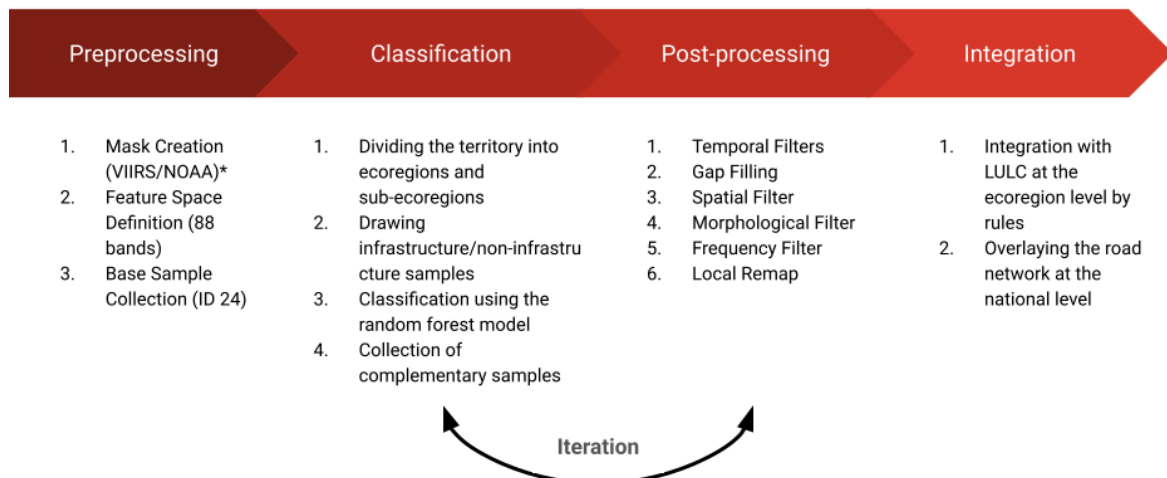
1. Introduction

1.1. Overview

Collection 2 of MapBiomas Chile incorporated the mapping of the Infrastructure class as a binary, cross-cutting layer across the national territory. This inclusion was conducted due to the frequent confusion with other non-vegetated land use classes, such as “Other non-vegetated areas” (25), “Rocky soils” (29), and “Sand, beach, and dunes” (23).

The Infrastructure class is composed of built-up surfaces and structures associated with large and small urban centers (towns), as well as continuous infrastructure areas larger than one hectare. It also includes industrial zones, road networks, and airports.

The general methodology can be seen in Figure 1.



*Annual global VIIRS nighttime lights dataset <https://doi.org/10.3390/rs13050922>

Figure 1: General Methodology.

2. Landsat Image Mosaics

2.1. Mosaic Composition

The mosaic composition used for the cross-cutting classification of the “Infrastructure” class relied on the image mosaics previously generated for the general Land Cover and Land Use classification of MapBiomas Chile Collection 2. The composition was made using surface reflectance satellite imagery with atmospheric correction from the Landsat 5, 7, and 8 sensors, generated annually from 1999 to 2024.

2.2. Feature Space

For the classification of this class, we used a subset of the variables derived from the overall mosaic for general LULC. The variables used as predictors are shown in table 1.

Table 1: Feature space, variables for the detection of infrastructure surfaces with the associated reducer.

Variable	Description	Reducer
blue	Landsat blue band	Median
green	Landsat green band	Median
red	Landsat red band	Median
nir	Landsat nir band	Median
swir1	Landsat swir 1 band	Median
swir2	Landsat swir 2 band	Median
soil	Soil fraction	Median
snow	Snow fraction	Median
cloud	Cloud fraction	Median
slope	Slope	Static topographic variable
ndvi	Formalized Difference Vegetation Index	Median
evi2	Enhanced Vegetation index	Median
ndwi	Normalized difference wet index	Median
mbi	Modified Bare Soil Index	Median
ndbi	Normalized Difference Built-up	Median
ndsi	Normalized Difference Snow Index	Median

Finally, a representative mosaic was created for each year, consisting of a total of 88 bands, based on the calculation of statistical reducers to generate the values for each pixel. These reducers correspond to: Median, Median of the dry season, Median of the wet season, Amplitude, Standard deviation, Minimum, Maximum, and Median texture. Only NDWI, MBI, NDBI and NDSI just have median reducers.

3. Classification

3.1. Definition of potential areas

We restricted the classification geographical extent to a mask built using a the VIIRS Nighttime Day/Night Annual Band Composite V2.2 product which is constructed from an annual time series of nighttime lights using monthly cloud-free radiance averages obtained from luminosity data collected by the sensor NASA/NOAA Visible Infrared Imaging Radiometer Suite (VIIRS) (Elvidge et al., 2021). The "average_masked" band representing the twelve-month average is specifically used to eliminate sporadic lights produced by the Northern Lights, fires or other isolated events. The used mask was built by selecting only the areas that had a pixel value greater than the value 0.4. This threshold was chosen based on iteration and revision of the area selected by the mask. This area corresponds to the potential infrastructure area, within which, we applied the random forest algorithm to classify the only two classes: Infrastructure and Others.

3.2. Definition of the Infrastructure class (ID: 24)

For collection 2, the infrastructure class (ID 24) is defined as urban and industrial areas, national and regional main roads, and other man-made structures such as seaports and airports. Mining and solar energy are not included.

All other coverage or uses that fall within the potential infrastructure area defined with the night lights were grouped into an auxiliary class called 'Others'.

3.3. Samples Collection

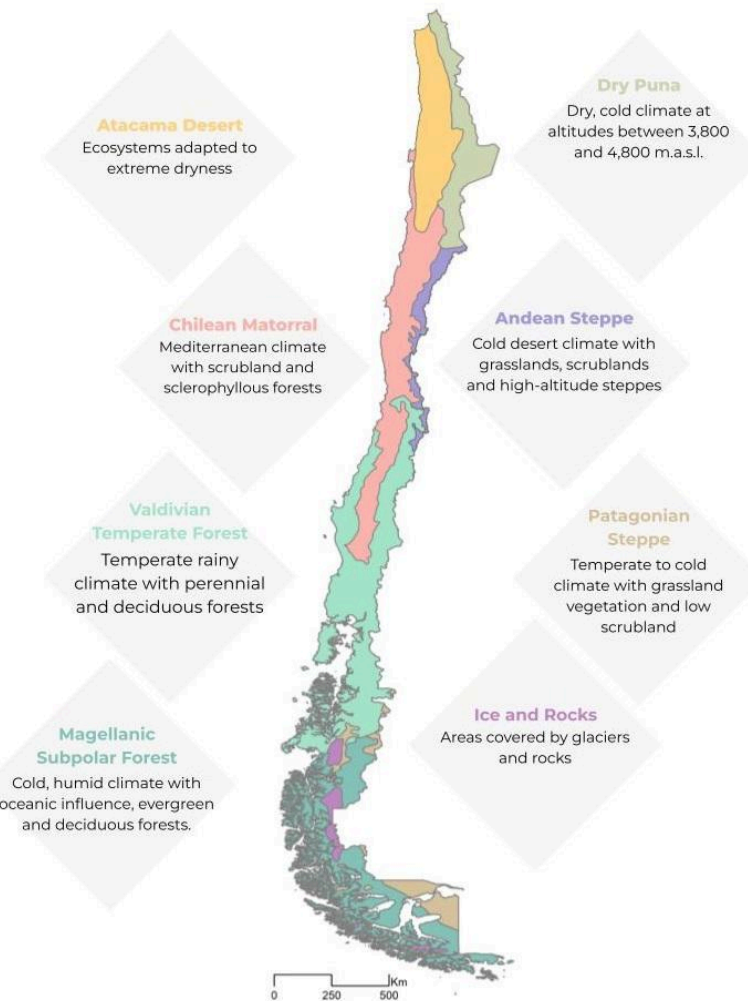
Infrastructure samples were collected through photointerpretation, manually drawing polygons using the 1998 image as a reference. These initial samples were only collected in large cities, avoiding including vacant lots, parks, squares, swimming pools and other structures typical of cities but that could increase confusion with other coverages in the polygons.

To train the samples of the class: 'Others', the training points used for the general classification of the LULC filter by the potential infrastructure areas were used.

3.4. Working areas

For Collection 2, ecoregions were used to stratify the national territory. This allowed for the collection of sampling points that explicitly considered the biophysical differences of the country's various geographic zones. Ecoregions are large geographic units that group natural communities with distinctive species compositions, ecological dynamics, and shared environmental conditions (Olson et al., 2001). We consider eight ecoregions: Dry Puna, Atacama Desert, Andean Steppe, Chilean Matorral, Valdivian temperate forests, Magellanic subpolar forests, Patagonian steppe and Ice and Rocks (Figure 2).

Figure 2: Chilean Ecoregions.



For the infrastructure layer, the ecoregions were also intersected by Chilean administrative political regions (level 2) to create a series of sub-ecoregions to facilitate the adjustment of the algorithms. This was also done to inspect the classification quality.

3.5. Classification Algorithm

Digital classification was performed in each working zone, year by year, using a Random Forest algorithm (Breiman, 2001) available in Google Earth Engine, running 100 iterations (random forest trees). The classification was carried out iteratively, increasing the complementary samples until an acceptable visual adjustment of the large cities in each area was achieved. Final classification was performed for all working zones and years with stable and complementary samples (Figure 3). All years used the same subset of samples and it was trained in the same mosaic of the year that was classified.

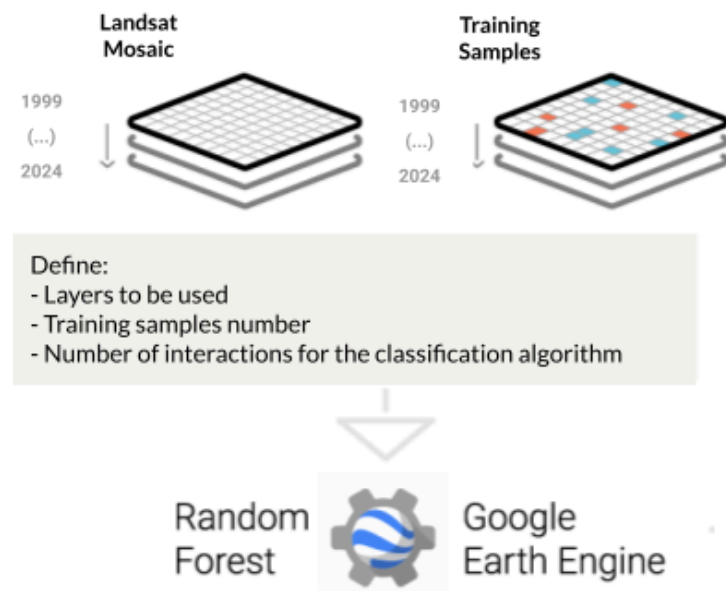


Figure 3: Representation of Landsat mosaic and training samples with two classes (red and blue).

4. Post Processing

As with the overall classification, the final Infrastructure classification results in each work area were improved by applying a set of temporal and spatial filters. First, temporal filters were applied to generate a more stable classification pattern over time, avoiding unexpected class variations during consecutive years or within a short period. Second, gap filter was applied to correct missing data and recover areas with missing information with pixels from earlier or later years. Third, spatial filters were applied to reduce the salt-and-pepper effect. In the Last step, a series of complementary filters was applied to reduce the remaining errors.

4.1. Temporal filters

To eliminate high-frequency variation in classification produced by differences in annual mosaic characteristics, additional spatial filters are applied. The first for a 3-year window that begins with the oldest classification to the most recent, without modifying the first and last year. In this window, when the target year (t) is not equal to the previous (t-1) and subsequent (t+1), the class of the previous year (t-1) is modified. This filtering is done in order of priority, changing and modifying the class with the biggest classification or noise problems, in this case "24" and then reviewing the most stable class, in this case "68". To the new classification, a temporal filter is applied that considers 4-year moving windows. This filter works the same as the previous one, but the condition is that the year (t) must be equal to the previous year (t-1) and different from the classification from 2 years before (t-2) and different from the year after (t+1). If the condition is met the classification is replaced by t-2. The iteration is carried out in order of priority from 1999 to 2024 without modifying the first and last year. Finally, a 5-year temporal filter was applied, whose operation is similar to the previous ones but the same years must be the 3 central ones (Figure 4).

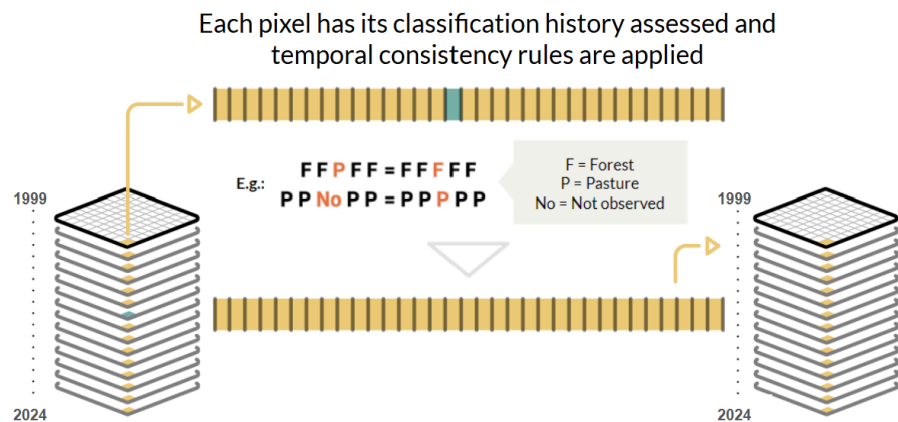


Figure 4: Temporal filter concept.

4.2. First and Last year filter

Extreme filters are applied exclusively to the temporal boundaries of the time series that is, the first and last years. For the first year, each pixel is compared with its class in the following year ($x+1$); for the last year, the comparison is made with the preceding year ($x-1$). The decision rule states that if a pixel's class in year x differs from that of its adjacent year, belonging to different thematic groups (i.e., anthropic vs. natural), the pixel in year x is reclassified to match the class of its neighboring year (Figure 5).

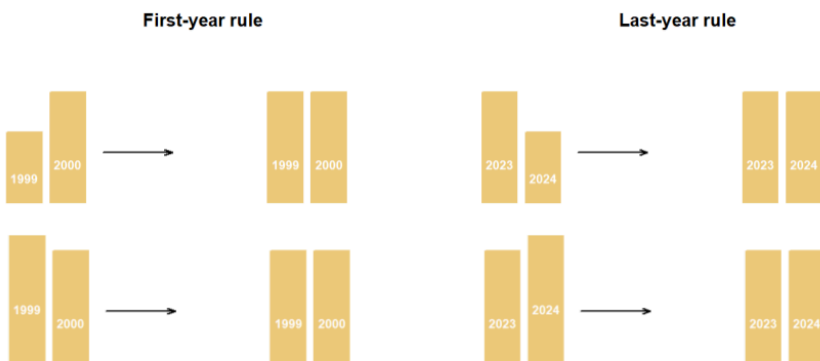


Figure 5: Extreme filter concept

4.3. Fill Gaps filter

A filter was applied to fill no-data pixels, or “gaps,” within the temporal series. Since, in principle, no-data values are not permitted, they were replaced with the temporally nearest valid classification.

In this procedure, if no valid future observation was available, the no-data pixel was replaced by its most recent valid class. Consequently, gaps should only persist in cases where a given pixel remained classified as no-data throughout the entire temporal domain.

4.4. Spatial filter

The spatial filter consists of eliminating areas where the number of pixels connected vertically, diagonally or horizontally is less than 11 pixels. This process is carried out by adding an auxiliary variable that contains for each pixel the number of connected pixels of the same class, then a moving window of 2x2 pixels is defined in which the mode is calculated and in each pixel that does not meet the condition of connected pixels, the original value is replaced by the mode of the classification in the neighborhood. This process is carried out independently each year.

SPATIAL FILTER

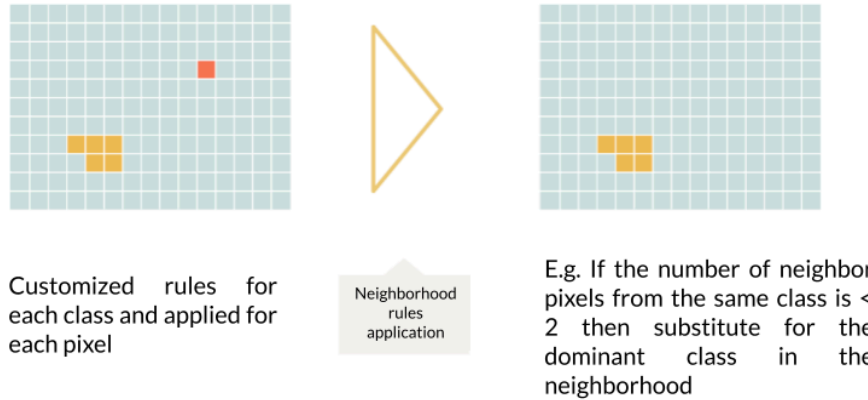


Figure 6: Spatial filter concept.

4.5. Frequency filter

The frequency filter was applied after the temporal filtering stage. The purpose of this filter is to reinforce temporal stability in land-cover types correcting residual fluctuations that may persist after the application of the temporal filters. This filter operates by analyzing the frequency of class occurrence for each pixel within the final years of the time series. For every pixel, the filter identifies the first year from which a given class becomes dominant or recurrent in the subsequent years. Once this year is detected, all following years are reassigned to the most frequent class within that period. In practice, this approach replaces sporadic or inconsistent class changes with the modal (most frequent) class observed in the stable portion of the series (Figure 7).

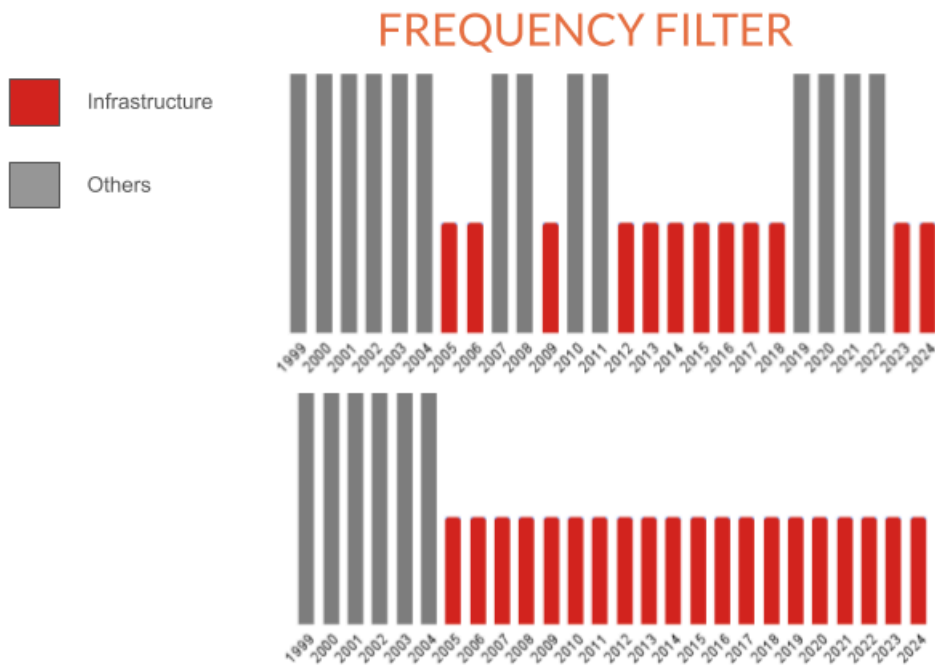


Figure 7: frequency filter concept.

4.6. Morphological filter

The morphological filter is a spatial post-processing operation applied to the classification maps to improve the geometric consistency of a class. It aims to remove small holes, isolated pixels, and internal irregularities that appear within class patches, ensuring a more homogeneous and realistic spatial representation. The procedure is based on a morphological closing operation, a common technique in image processing used to fill small internal gaps while preserving the general shape of the features.

The annual classification is first converted into a binary mask identifying all pixels corresponding to the class of interest, over this binary mask, the closing operation is performed by applying a dilation followed by an erosion. The dilation temporarily expands the extent of the class areas, allowing small gaps between neighboring pixels to be filled. Subsequently, the erosion step contracts the expanded areas, restoring the external shape of the polygons while maintaining the newly filled internal pixels. Both operations are applied using a diamond-shaped structuring element with a radius of one pixel, equivalent to 30 meters.

4.7. Remap

When localized errors persist that are not resolved by spatial or temporal filters, a manual remapping is applied as a final step. This procedure allows replacing specific classes within defined areas of interest and, if needed, restricting changes to particular years, while honoring a priority order for edits. The operation is configured by specifying the source class (*from*) and the target class (*to*); the algorithm affects only those pixels within the AOI that meet this condition. This intervention is used sparingly and in a controlled manner to correct specific cases that automatic filters could not stabilize.

5. Integration

After applying all filters, the classifications for each sub-ecoregion are assembled to reconstruct the entire national territory. This layer is then integrated into the overall LULC map by applying replacement rules for class 24 (Infrastructure) by zone:

- From Arica y Parinacota region to the north of the Copiapó river class Infrastructure replaces 23, 25, 29, 12, and 66.
- From the south of the Copiapó river to the southern boundary of the Ñuble region class Infrastructure replaces 23, 25, 29, 18, 12, 66, and 9.
- From the northern boundary of the Biobío region to the Magallanes region class Infrastructure replaces 23, 25, 29, 18, 66, 15, 59, 9, 33, and 34.

These rules were defined through inspection and visual validation, identifying in each zone which classes most frequently occupied cities, airports, or seaports areas when class Infrastructure was not included in the original classification, in order to ensure spatial coherence in the final product.

In Table 2 it's a summary of the legend with its corresponding pixel identification.

Table 2: List of Collection 2 classes

Natural/Anthropic	Class name	Pixel id
	1. Forest formation	1
Natural	1.1. Forest	3
Natural	1.1.1 Primary Forest	59
Natural	1.1.2 Secondary Forest	60
Natural	1.1.3 Dwarf forest	67
	2. Natural non forest formation	10
Natural	2.1. Wetland	11
Natural	2.2. Grassland	12
Natural	2.3. Steppe	63
Natural	2.4. Shrubland	66
Natural	2.5. Rocky Outcrop	29
	3. Farming and silviculture	14
Anthropic	3.1. Silviculture	9
Anthropic	3.2. Agriculture	18
Anthropic	3.3. Pasture	15
	4. Non-vegetated area	22
Anthropic	4.1. Infrastructure	24
Natural	4.2. Beach, Dune and Sand Spot	23
Natural	4.3. Salt Flat	61
Natural	4.4. Other non-vegetated area	25
	5. Water bodies	26
Natural	5.1. River, lake or ocean	33
Natural	5.2. Ice and snow	34
	6. Not observed	27

The last part to complete the infrastructure layer was to add Chile's road network. For this, the vector map of main regional and national roads of Chile¹ was converted to raster and joined year by year with the infrastructure classification

¹ https://mapas.mop.gov.cl/red-vial/Red_Vial_Chile.zip

6. References

- Breiman, L. (2001). Random forests. *Machine learning*, v. 45, n. 1, p. 5-32.
- Elvidge, C.D, Zhizhin, M., Ghosh T., Hsu FC, Taneja J. (2021). Annual time series of global VIIRS nighttime lights derived from monthly averages:2012 to 2019. *Remote Sensing* 2021, 13(5), p.922, doi:10.3390/rs13050922 doi:10.3390/rs13050922.
- Olson, D. M., Dinerstein, E., Wikramanayake, E. D., Burgess, N. D., Powell, G. V. N., Underwood, E. C., D'Amico, J. A., Itoua, I., Strand, H. E., Morrison, J. C., Loucks, C. J., Allnutt, T. F., Ricketts, T. H., Kura, Y., Lamoreux, J. F., Wettengel, W. W., Hedao, P., Kassem, K. R. 2001. Terrestrial ecoregions of the world: a new map of life on Earth. *Bioscience* 51(11):933-

